Journal for Geometry and Graphics
Volume 13 (2009), No. 2, 187–194.

Connectivity and a Diffusion Limited Aggregation Digital Image Magnification Technique

Gary Greenfield

Mathematics and Computer Science, University of Richmond
Richmond, Virginia 23173, USA
email: ggreenfi@richmond.edu

Abstract. This paper first reviews a method for using diffusion limited aggregation (DLA) to make non-photorealistic enlargements of digital images that combine characteristics of mosaic rendering with space-filling curve rendering. The issue we then address is the topological connectivity of the graphs induced by pixel adjacencies in our image enlargements. In particular, we examine the size of the largest connected component and the number of connected components that occur in the induced graphs in order to assess empirically how close the induced graphs are to being simply connected.

Key Words: image enlargement, diffusion limited aggregation, connected graph

MSC 2000: 68U05

1. Introduction

Image magnification obtained by using a low resolution image is a classical digital image processing challenge that motivates half toning and (colour) dithering. Although Ken Knowlton [4] pioneered some of the earliest non-photorealistic pixel by pixel, scanline magnification techniques for addressing this challenge, currently the most popular pixel by pixel method is *Photomosaics* by R. Silvers [9]. An alternative non-photorealistic image magnification technique invokes curve fitting using only a carefully selected subset of source image pixels. Prominent examples of this technique include *TSP Art* by Kaplan and Bosch [3], which uses solutions to the traveling salesperson problem (TSP) to fit curves to sampled image points, and the space filling curve approach used by K. Mitchell [7].

In this paper we combine pixel magnification and curve fitting by first using *diffusion limited aggregation* (DLA) to form *"dendrites"* for pixel by pixel magnification and then again using DLA to glue dendrites of pixels together in such a way that they almost yield a space filling curve. By "almost" we mean that the induced pixel adjacency graph has a

ISSN 1433-8157/$ 2.50

connected component that accounts for up to 99 percent of the magnified image's dendritic pixels. More precisely, in general, our method yields a small number of "large" connected components, and that small number decreases as the magnification factor increases. This paper follows upon the author's related work [1, 2]. For a completely different approach to using DLA in non-photorealistic rendering see Long [6].

Stated formally, our objective is to magnify a source image S with pixel dimensions $w \times h$ to obtain an enlarged image D with pixel dimensions $pw \times ph$ that is surrounded by a border of white pixels of width p in such a way that the filled or coloured pixels of D are simply connected.

2. Magnification Algorithm

2.1. DLA simulation

Diffusion limited aggregation (DLA) is a simulation technique used to model dendritic growth. The method of Kobayashi et al. [5] aggregates particles to a central seed by releasing particles one at a time a fixed distance away from the growing dendrite and allowing them to undergo a random walk for a fixed number of time steps until they either adhere to the existing dendrite, wander out of range, or their time limit expires. An example of the typical dendritic structure this method yields is shown in Fig. 1. We modify the method slightly by replacing the taxicab distance metric with the supremum distance metric so that neighborhoods of central seeds will be squares instead of diamonds.

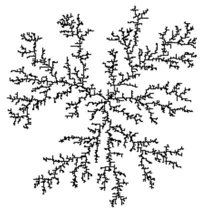

Figure 1: An example of a DLA dendrite produced using the basic Kobayashi et al. algorithm

2.2. Three-pass magnification

Let the magnification factor $p > 3$ be odd. Writing $p = 2k + 1$, our three pass image magnification scheme identifies pixel (i, j) of the source image S with the $2k \times 2k$ pixel neighborhood N of radius k centred at pixel $\big(p(i+1)+k,\ p(j+1)+k\big)$ of the destination image D that is defined by the supremum distance. The first two passes independently place a dendrite of radius k emanating from the centre of each neighborhood N of D. In the third and final pass, for each neighborhood N of D we initiate a random walk around the edges of the four cardinally adjacent neighborhoods of N in search of a dendrite particle. If one is found, we use it as a central seed and grow a dendrite a radius k emanating from it, but we only aggregate particles if they lie in N. In this way a neighboring dendrite flows back into N.

2.3. Artistic considerations

To more faithfully reproduce the image when it is magnified, and to help nullify image fading due to the presence of white pixels that are not visited during DLA aggregation, the three pass algorithm also uses a stickiness, or fluffiness, factor s, where $0 \leq s \leq 1$, which stochastically determines how often a particle in motion aggregates when it encounters an existing DLA structure. By setting s to be the luminance value of source image pixels, the magnification algorithm more accurately reproduces the luminance profile in the enlargement because darker source pixels then spawn more aggregated particles.

2.4. An example

Figure 2 shows a 194×259 pixel source image down sampled from a 1944×2592 pixel photo of a giraffe taken by J. Ward.

Figure 2: The 194×259 down sampled source image giraffe (left) and 2156×2871 DLA based enlargement (right). Not to scale.

3. Enlargement Connectivity

Henceforth, as a test image, we use the 158×158 gray scale *Lena* image shown in Fig. 3. For $p = 7$, which gives $p + 158p + p = 1120$, Fig. 3 also shows the 1120×1120 magnified image, while Fig. 4 shows detail from the lower left corner of this image, DLA deposited 599809 particles. Taking these as the vertices of a pixel adjacency graph, if we define adjacency solely on the basis of the four cardinal compass directions, there are 805069 edges yielding 530 connected components. The largest component contains 582357 vertices or 97% of the vertices; no other component contains more than 571 vertices; and only 30 components contain more than 100 vertices. If we also include edges to account for diagonal pixel adjacency, which seems more natural if our goal is to determine the number of connected components our visual system would recognize, then the resulting graph has 1487762 edges, and now there are only 124 components with the largest component having 597483 vertices, or 99.6% of the vertices. Moreover, no other component contains more than 45 vertices!

Figure 3: The 158×158 test *Lena* source image (left) and 1120×1120, $p = 7$ DLA based enlargement (right). Not to scale.

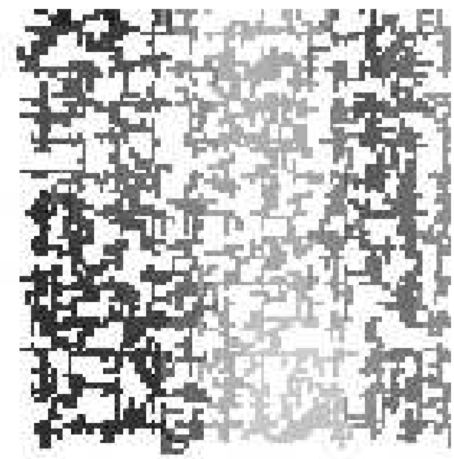

Figure 4: Lower left hand corner of the $p = 7$ *Lena* enlargement

4. Empirical Results

Since topological connectivity and the number of connected components depend on how likely a dendrite will reach the boundary of a neighboring block of pixels, as well as the total number of blocks of pixels, one would expect that as the magnification factor increases and the blocks become larger, the size of the largest connected component will decrease. Arguing on the basis of random graphs, if after the first two passes there are wh connected components i.e., disconnected subgraphs, and we now add at most wh edges connecting these subgraphs in such a way that a subgraph can be connected to at most four of its immediately adjacent components by one of these edges, then one would expect a large central "core" component to arise with many smaller components congregating near the boundary.

In other words, by viewing the enlarged blocks of pixels as vertices in their own right, by contraction, we are concerned with the connectivity of a very special kind of random graph: one all of whose vertices lie on a two dimensional $w \times h$ grid; all of whose edges have unit length; and all of whose vertices have radius at most one. Since a formal analysis is difficult (for a partial analysis of the one-dimensional case, see Noshiro et al. [8]) we resort to an empirical verification that large connected components will result. To this end, by using the test *Lena* image, we make p-fold enlargements using successively smaller down sampled *Lena* source images in such a way that each enlargement is approximately 1500×1500 pixels. Henceforth we will always include edges (necessarily of length $\sqrt{2}$) in our graph for each pair of diagonally adjacent aggregated particles in our enlargements.

Table 1 shows the resulting empirical data. In Table 1, the magnification factor is p, the down sampled source image width (equal height) dimension in pixels is w, the number of vertices in the induced enlargement graph is V, the number of edges is E, the number of connected components is C, and the number of pixels/vertices in the largest component is L.

Table 1: Empirical data from a sequence of 1500×1500 pixel p-fold *Lena* enlargements

p	w	V	E	C	L
9	165	995118	2451908	323	982571
11	135	940303	2316570	361	913937
13	115	911963	2243271	331	862442
15	100	886618	2181885	326	804341
17	85	796465	1956077	278	687384
19	75	752452	1841225	268	435163
21	70	786544	1924211	251	400411
23	65	794964	1938561	251	467158
25	60	784229	1908339	242	225046
27	55	752637	1825291	253	196541
29	50	708330	1713313	225	89823
31	45	643828	1553037	177	109681
35	40	632336	1519907	162	65545
39	35	584407	1401034	149	61221
45	30	549257	1307716	121	54752
55	25	540408	1273111	107	24678

The results are as expected. Although the number of vertices in the largest component as a percentage of the total number of vertices drops from 98.7% to 9.9%, in all cases there are a small number of very large components. For example, in the $p = 45$ case, where the largest component accounts for only 4.6% of the total number of vertices, if the $549257 - 54742 = 494505$ unaccounted for vertices were evenly distributed among the remaining 120 components, the average component would have 4120 vertices. But examining the sizes of the components reveals that there are four additional components — of sizes 42152, 27613, 23320, 20657 — that also have more than 20000 vertices so the average number of pixels in most of the remaining components is much, much smaller than this worse case estimate.

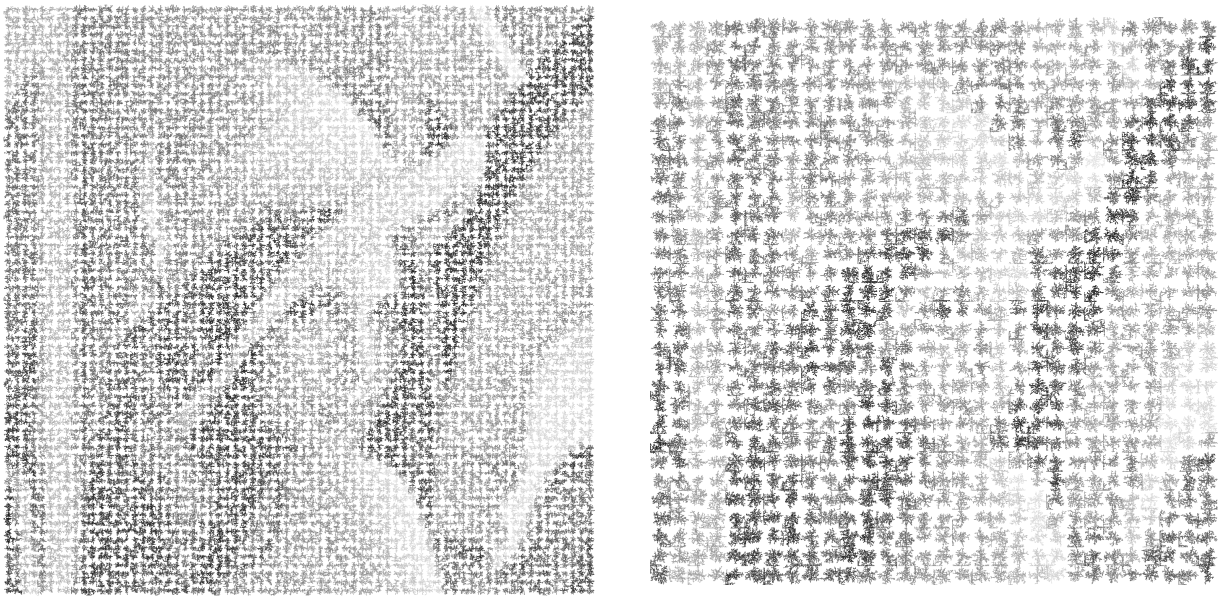

Figure 5: *Lena* enlargement using magnification factor $p = 21$ (left) and $p = 45$ (right)

More importantly, by comparing the $p = 7$ enlargement in Fig. 3 with the $p = 21$ enlargement and the $p = 45$ enlargement both shown in of Fig. 5, one becomes quickly convinced that it is difficult for the eye to discern that any of the *Lena* enlargements have as many components as they really do. Using the data in Table 1, the Pearson linear correlation coefficient is 0.876 for the variables p and L, while for the variables p and C it is 0.963. Using p as the independent variable, the equation of the regression line predicting the size of L is $L = -23772.7p + 1013911$. It does not appear to be very useful.

One anomaly that does stand out in Table 1 is the size of the largest component for the $p = 29$ enlargement. This does seem to be an exceptional case. Table 2 shows the empirical results obtained from six different $p = 29$ enlargements. Perhaps the variability in C, the size of the largest component, is caused by parameter settings in the underlying DLA simulation. On the other hand the average number of vertices for these six largest components is 120549 which meshes nicely with Table 1. Figure 6 shows the two enlargements corresponding to the examples from Table 2 with the maximal and minimal largest connected components. To the eye, there is little discernable difference between them.

Table 2: Empirical data from six 1500 × 1500 pixel $p = 29$ *Lena* enlargements

V	E	C	L
709525	1718086	223	229421
708885	1716264	209	170485
708219	1713060	217	104744
707165	1709846	223	75486
707732	1713435	238	73300
706889	1709486	229	69858

5. Conclusions

We have presented an algorithm for image enlargement from thumbnail images based on diffusion limited aggregation to obtain a non-photorealistic image style that combines mosaic and space-filling curve techniques. Since the method is stochastic, we examined how close colored pixels in the enlargement come to representing a connected curve by examining the number of connected components and their sizes in the induced pixel adjacency graph.

We used empirical data to reveal that the graph is dominated by large connected components, and to try to demonstrate that the human visual system cannot distinguish between the individual components. This helps to confirm that the algorithm does minimize both the blocky artifacts persistent in mosaic enlargements and the angular geometric artifacts persistent in space filling curve enlargements.

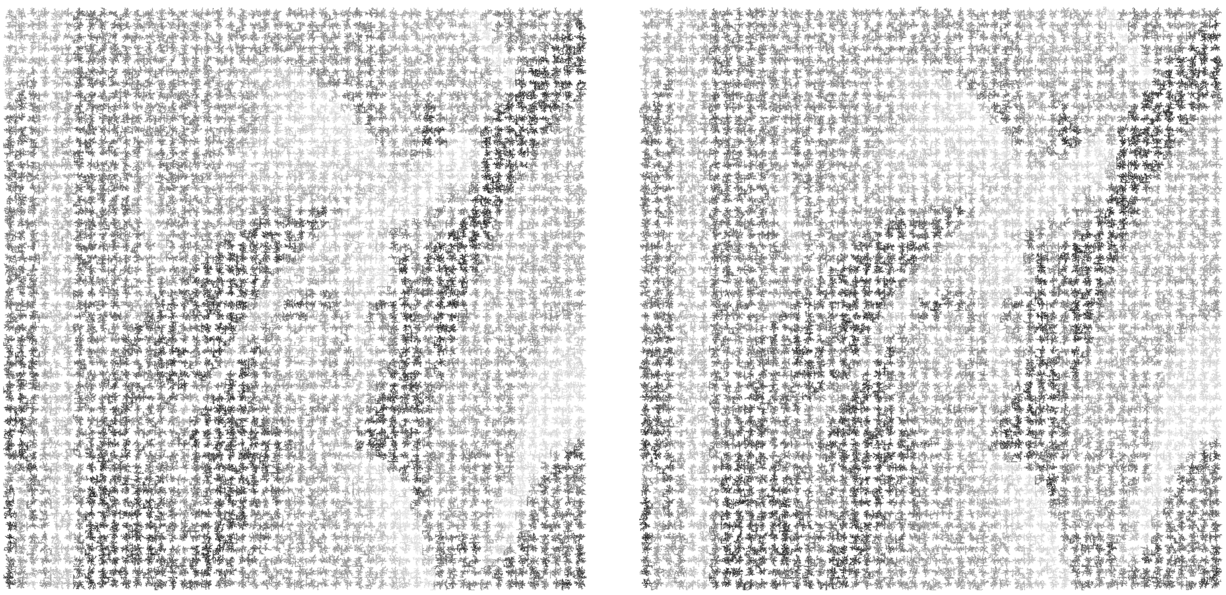

Figure 6: Two of the $p = 29$ *Lena* enlargements referred to in Table 2. Left, the one whose largest connected component has 229421 vertices/pixels. Right, the one whose largest connected component has 69898 vertices/pixels.

References

[1] G. Greenfield: *Composite diffusion limited aggregation paintings*. Bridges Donostia: Bridges 2007: R. Sarhangi, J. Barrallo (eds.), *Mathematical Connections in Art, Music and Science*, 15–20 (2007).

[2] G. Greenfield: *Composite digital mosaics using duotone tiles*. Bridges 2009 Conference Proceedings, C. Kaplan, R. Sarhangi (eds.), 155–162 (2009).

[3] C. Kaplan, R. Bosch: *TSP art*. Renaissance Banff: Bridges 2005: R. Sarhangi, R. Moody (eds.), *Mathematical Connections in Art, Music and Science*, 301–308 (2005).

[4] K. Knowlton: `http://www.knowltonmosaics.com/` (accessed March 11, 2008).

[5] Y. Kobayashi, T. Niitsu, K. Takahashi, S. Shimoida: *Mathematical modeling of metal leaves*. Mathematics Magazine, **76**(4), 295–298 (2003).

[6] J. Long: *Modeling Dendritic Structures for Artistic Effects*. M.Sc. Thesis, University of Saskatchewan, Saskatoon 2007.

[7] K. Mitchell: *Techniques for artistically rendering space-filling curves*. Bridges 2002 Conference Proceedings, R. Sarhangi (ed.), 277–283 (2002).

[8] A. Noshiro, T. Yoshikawa, M. Kurihara: *Analysis for connectivity of fixed radius random graph with the one-dimensional uniform distribution*. Transactions of Information Processing Society of Japan **46**(10), 93–102 (2005).

[9] R. Silvers: *Photomosaics*. Henry Holt and Company, New York 1997.

Received August 5, 2008; final form September 19, 2009